Structure and vibrational spectroscopy of methanesulfonic acid hydrazide: an experimental and theoretical study†

Andrea Ienco,[a] Carlo Mealli,*[a] Paola Paoli,[b] Nicolay Dodoff,[c] Ziya Kantarci[d] and Nurcan Karacan[e]

[a] *Istituto per lo Studio della Stereochimica ed Energetica dei Composti di Coordinazione, CNR, Via J. Nardi 39, 50132 Firenze, Italy. E-mail: mealli@fi.cnr.it*
[b] *Dipartimento di Energetica "Sergio Stecco", Università di Firenze, Via di S. Marta 3, 50139, Firenze, Italy*
[c] *Institute of Molecular Biology, Bulgarian Academy of Sciences, Acad. G. Bonchev Street, Block 21, 1113 Sofia, Bulgaria*
[d] *Department of Physics and* [e] *Department of Chemistry, Faculty of Science and Art, Gazi University, Teknik Okullar, 06500 Ankara, Turkey*

Received (in Montpellier, France) 30th July 1999, Accepted 30th September 1999

A comprehensive study of the molecule of methanesulfonic acid hydrazide (MSH) is presented. The X-ray structure shows that in the crystal two centrosymmetrically oriented MSH molecules are held together by N–H···N hydrogen bonding interactions. This feature is unprecedented for the known arylsulfonic hydrazide analogues. The energetics of the various MSH staggered conformers and the stabilisation due to dimerisation are evaluated by HF *ab initio* calculations. Moreover, the pathways that interconvert the conformers as well as their enantiomers are outlined. The transition states between conformers correspond to the eclipsed conformation about the S–N linkage while those between enantiomers require planarisation of the N atom bound to sulfur. Some interconversions require two steps and two barriers to be bypassed. The IR and Raman spectra of MSH have been recorded and a normal coordinate analysis (NCA) has been carried out. The assignments have been double-checked through the *ab initio* calculated frequencies. The latter techniques also allow evaluation of the normal modes of vibration due to interacting MSH monomers, which can be experimentally detected.

Sulfonamides are a well-known class of potent chemiotherapeutic agents with versatile activity,[1] including an antitumor effect.[2] The methanesulfonamide residue has also appeared as a suitable pharmacophoric equivalent to replace functional groups in drug design.[3] On the other hand, many compounds containing a hydrazine fragment, such as carboxylic acid hydrazides, have shown cytostatic activity.[4] Methanesulfonic acid hydrazide, $CH_3SO_2NHNH_2$ (MSH), is the simplest organic representative of compounds containing both sulfonamide and hydrazine fragments. Although this compound was first synthesised many years ago,[5] it is still poorly characterised, both structurally and spectroscopically. One could expect a non-trivial conformational behaviour of this molecule due to the presence of adjacent lone electron pairs and polar bonds, a feature that is known as a frequent source of "conformational anomalies".[6]

Here we report the X-ray structure of MSH, the *ab initio* optimised structures of various conformers, as well as the interpretation of the vibrational spectra of the compound on the basis of *ab initio* computed frequencies and normal coordinate analysis (NCA).

Experimental

Starting compounds and materials

Methanesulfonyl chloride and hydrazine hydrate (p.a., Merck) were used without purification. Diethyl ether (ether), ethyl acetate and the remaining solvents used were purified according to routine procedures.[7] Thin layer chromatograms (TLC) were performed on silicagel on glass plates (particle size 5–17 μm, layer 250 μm) from Sigma. The samples were applied as methanolic solutions, the chromatograms were developed ascendingly with the solvent system benzene–acetonitrile (15 : 18.5) saturated with water, and the spots were visualised in iodine vapour atmosphere.

Preparation of MSH

MSH was prepared by reacting methanesulfonyl chloride and hydrazine hydrate followed by continuous ether extraction of the product, according to the procedure of Powell and Whiting,[8] slightly modified to improve the yield and purity of the target compound. The continuous extraction conditions from ether were optimised. The syrupy material obtained was dried azeotropically with benzene. In this manner a crystalline product (80%) was obtained and recrystallised from boiling ethylacetate. After cooling (−5 °C) colourless prismatic crystals were deposited; these were dried *in vacuo* over P_2O_5 and stored in a dry atmosphere. The melting point was 50.5 °C (uncorrected, Kofler microscope). The product was TLC homogeneous, with $R_f = 0.55 \pm 0.03$. ^{1}H NMR (DMSO-d_6): δ 2.88 (s, 3H, CH_3); 4.32 (s, 2H, NH_2); 7.67 (s, 1H, NH).

Spectroscopy

The ^{1}H NMR spectrum of a DMSO-d_6 solution of MSH was registered on a Bruker WM-400 spectrometer (400 MHz) using tetramethylsilane as internal standard. D_2O exchange

† *Non-SI units utilised*: 1 kcal = 4.184 kJ; 1 au ≈ 2.63 × 10^6 J mol^{-1}.

was applied to confirm the assignment of the NH and NH_2 signals.

The infrared (IR) spectra of MSH were recorded on a Bruker IFS113 spectrophotometer using three techniques: (*a*) CsI disks (4000–150 cm^{-1}), (*b*) liquid film (melt) between CsI plates (4000–150 cm^{-1}), and (*c*) acetonitrile solution in a KBr cell (4000–3150 cm^{-1}). A partially deuterated specimen of MSH was prepared by dissolving MSH (*ca.* 30 mg) in *ca.* 1 ml of methanol-d_4 and evaporating the solvent *in vacuo*, this operation being repeated three times. Finally the sample was dried in a vacuum desiccator over P_2O_5. The IR spectrum of the deuterated sample was taken as a liquid film (see above).

The Raman spectrum of a solid sample of MSH was obtained in the range 4000–70 cm^{-1} with a Jobin–Yvon U1000 spectrometer calibrated against the laser plasma emission lines. The 488 nm line of a Spectra-Physics Model 2016-4S argon gas laser was used for excitation.

X-Ray structure data collection and processing

Parallelepiped crystals of MSH were obtained from ethyl acetate–ether solution after one week cooling at −25 °C. A summary of crystal and intensity data, collected on an Enraf-Nonius CAD4 diffractometer, is presented in Table 1. The cell constants were determined by using 25 reflections in the range $8 < \theta < 14°$. Intensity data were corrected for Lorentz polarisation effects. In view of the small absorption coefficient (0.569 mm^{-1}) no absorption correction was applied. The structure was solved by using the package SIR92,[9] which gave the positions of all the non-hydrogen atoms. The refinement was carried out with the programs SHELXL93.[10] The hydrogen atoms were located from Fourier difference maps at advanced stages of the refinement and then refined with individual isotropic temperature factors. Atomic scattering factors were those reported by Cromer and Waber[11] with anomalous dispersion corrections. The refinement was considered terminated for an *R* factor of 0.06. Although the wR_2 factor appears somewhat high (0.21), no unusual features were observed in the final ΔF map or in the statistics of F_o/F_c. The e.s.d.s on bond distances are on the order of thousandths of Å, and of hundredths of Å whenever the hydrogen atoms are involved. Table 2 reports molecular bond lengths and angles. The structure factors are available on request from the authors.

CCDC reference number 440/148. See http://www.rsc.org/suppdata/nj/1999/1253/ for crystallographic files in .cif format.

Ab initio computational details

All of the staggered MSH conformers were optimised with no symmetry constraint by means of *ab initio* calculations at the HF/6-31G(d) and HF/6-311++G(d, p) levels by using the package Gaussian94.[12] The transition states connecting different isomers (conformers and/or enantiomers) were localised by using different algorithms of the package Gaussian94. In any case, the nature of each model (minimum or transition state) was substantiated by the evaluation of vibrational frequencies. Table 3 lists the total energy of the computed conformers and transition states, which are all conveniently schematised in Fig. 1.

As another approach, a rigid potential energy scan was performed with independent rotations of MSH about the axes N(1)–N(2) and S–N(2) in the full ranges of 0–360° with single steps of 30° at the HF/6-31G(d) level. The molecular geometry chosen was essentially that of the conformer **1** (or **1′**), which is the absolute energy minimum.

Finally, in order to reproduce the dimer observed in the experimental X-ray structure, a model of MSH doubled through a centre of inversion (C_i symmetry) was optimised at the HF/6-311++G(d, p) level of theory. The reliability of the optimisation was again confirmed by the frequencies.

Table 1 Crystal data and structure refinement for $CH_3SO_2NHNH_2$

Chemical formula	$CH_6N_2O_2S$
Formula weight	110.14
Crystal system	Triclinic
Space group	$P\bar{1}$
a/Å	5.427(5)
b/Å	5.828(5)
c/Å	7.649(5)
α/°	91.970(5)
β/°	95.840(5)
γ/°	107.410(5)
U/Å^3	229.1(3)
Z	2
T/K	293
μ/mm^{-1}	0.569
Reflections collected	1728
Independent reflections	1341 [*R*(int) = 0.0958]
Final *R* indices [$I > 2\sigma(I)$]	$R_1 = 0.0600$, $wR_2 = 0.2130$
R indices (all data)	$R_1 = 0.0704$, $wR_2 = 0.2249$

Table 2 Comparison of experimental and optimised geometrical parameters (the latter refer to the dimeric unit) in Å for bond lengths and degrees for bond angles

	Experimental	Calculated
S–O(2)	1.431(2)	1.422
S–O(1)	1.436(3)	1.424
S–N(2)	1.624(3)	1.635
S–C	1.750(3)	1.774
N(2)–N(1)	1.420(4)	1.393
N(2)–H(3)	0.79(4)	1.000
C–H(4)	0.85(4)	1.082
C–H(5)	0.90(6)	1.082
C–H(6)	0.93(5)	1.081
N(1)–H(1)	0.72(7)	1.002
N(1)–H(2)	0.96(4)	0.999
O(2)–S–O(1)	119.0(2)	121.7
O(2)–S–N(2)	106.52(14)	106.65
O(1)–S–N(2)	105.03(14)	105.61
O(2)–S–C	107.7(2)	107.26
O(1)–S–C	108.3(2)	107.54
N(2)–S–C	110.1(2)	107.34
N(1)–N(2)–S	120.2(2)	121.67
N(1)–N(2)–H(3)	106(3)	114.38
S–N(2)–H(3)	121(3)	116.25
S–C–H(4)	107(3)	109.71
S–C–H(5)	103(4)	106.69
H(4)–C–H(5)	96(4)	109.55
S–C–H(6)	109(3)	109.01
H(4)–C–H(6)	119(4)	111.50
H(5)–C–H(6)	121(5)	110.26
N(2)–N(1)–H(1)	112(6)	112.56
N(2)–N(1)–H(2)	110(3)	108.88
H(1)–N(1)–H(2)	89(5)	108.93

Table 3 Total energies (au) of the computed species (conformers and TS) and of the dimer species. The number of imaginary frequencies N_{imag} is given in parentheses

	E(HF/6-31G(d))// (HF/6-31G(d)) (N_{imag})	*E*(HF/6-311++G(d,p))// (HF/6-311++G(d,p)) (N_{imag})
1	−697.376 79 (0)	−697.490 97 (0)
2	−697.372 11 (0)	−697.4869 (0)
3	−697.366 79 (0)	−697.481 54 (0)
4	−697.371 75 (1)	−697.486 64 (1)
5	−697.363 83 (1)	−697.477 90 (1)
6	−697.366 50 (1)	−697.481 24 (1)
7	−697.358 73 (1)	−697.474 33 (1)
Dimer		1394.986 37 (0)

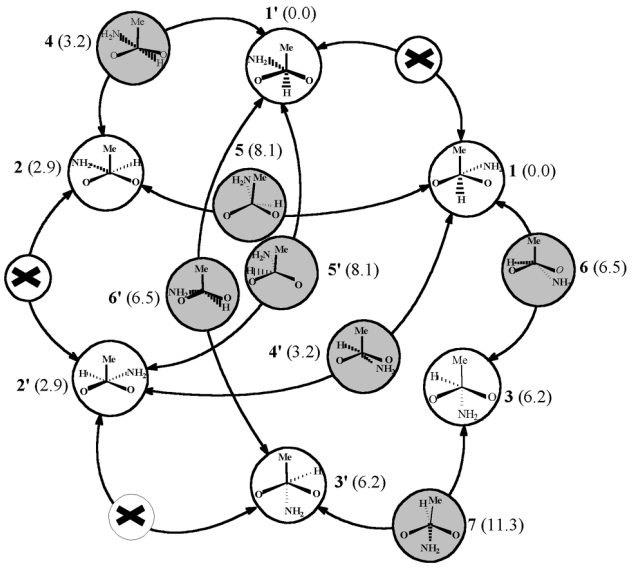

Fig. 1 Newman projections of the computed species (conformers, enantiomers and TS). Double-headed arrows connect pathways between conformers and/or enantiomers. Bold numbering identifies the computed species, in parenthesis the relative energy contents [HF/6-31G(d) level, kcal mol^{-1}] are reported.

Normal coordinate analysis. NCA of a single MSH molecule was performed in a harmonic generalised valence force field using the program MOLVIB 6.0 of Sundius.[13–15] Since it appears interesting to compare the frequencies obtained with the latter method with those derived from the *ab initio* study, the same MSH coordinates obtained from the optimisation of the C_i dimer were adopted. However, the NCA was limited to only one-half of the dimer.

Results and discussion

Crystal structure

In the crystal structure, two $CH_3SO_2NHNH_2$ units self-assemble in a centrosymmetric arrangement *via* the hydrogen bonds highlighted in Fig. 2. Selected bond distances and angles are presented in Table 2. It is evident that each molecule uses the lone pair of the terminal NH_2 group to interact with the H(3) atom bound to the N(2) atom of the other molecule [distance N(1)–H(3)′ = 2.36(4) Å, angle N(1)–H(3)′–N(2)′ = 139(4)°]. Although quasi-planar, the resulting six-membered ring is best described as a chair because the planes H(3)–N(2)–N(1) and its centrosymmetric equivalent are bent at *ca.* 15° with respect to the N(1)′–H(3)–N(1)–H(3)′ rectangle. Besides the major N–H···N bonding responsible for the dimerization of MSH, additional hydrogen bonding involves, both intra- and inter-molecularly, the two H atoms bound to N(1) and the sulfonyl oxygen atoms [distances range from 2.12(4) to 2.73(4) Å]. Interestingly, the present structure is the first example of a sulfonyl hydrazine containing an alkyl substituent. Four other structures with aryl substituents (2-naphthyl,[16] 4-toluyl,[17] and phenyl[17–19]) have been reported but none features the dimeric arrangement found for MSH. On the other hand, hydrazine itself forms analogous hydrogen-bonded six-membered rings.[20] While the bond distances between the heavier atoms are all similar in sulfonyl hydrazine molecules [we observe here the typical values of 1.420(4), 1.624(3) and 1.433(3) Å for the N(1)–N(2), N(2)–S and S–O (ave) bonds, respectively], the hydrogen bonding network seems to have a peculiar effect on the geometry of MSH. Thus, the N(1)–N(2)–S angle opens up significantly to a value of 120.2(2)° whereas, in the reference compounds, it is never larger than 115°. In any case, exact sp^2 hybridisation is not attained by the N(2) atom as the bound H(3) atom deviates by as much as 0.46(4) Å from the NNS plane. Table 4 compares important structural parameters between the experimental MSH structure and the known structural analogues.[16–19] In this table the geometries of the computed conformers (*vide infra*) are also reported.

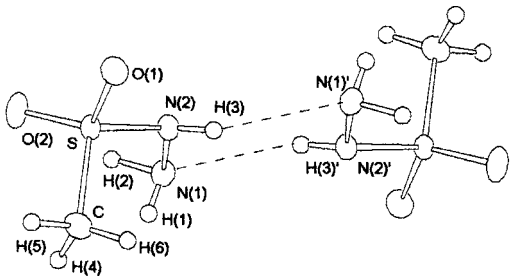

Fig. 2 ORTEP drawing showing the hydrogen bonding network connecting two $CH_3SO_2NHNH_2$ units.

Theoretical studies of the molecular conformation

Hartree–Fock (HF) calculations, carried out for both the isolated molecule and the dimer, confirm that intermolecular interactions affect the geometry of the MSH unit. In fact, the computed N···H contacts are comparable with the experimental structure (2.31 *vs.* 2.36 Å) and the trend towards opening of the N–N–S angle is fully confirmed (121.7°).

The Newman projections of the conformers **1**, **2** and **3** (as well as their enantiomers **1′**, **2′** and **3′**) are schematically presented in Fig. 1 (white circles) together with the detected tran^{-1}, sition states (shaded circles). The energies [kcal

Table 4 Comparison of selected geometrical parameters for MSH and the known structures of sulfonyl hydrazine molecules (indicated by the Cambridge Structural Database refcodes). The optimised geometries of the three staggered conformers and of the dimeric species are also reported

	N(1)–N(2)–S	Σ Angle N(1)	Σ Angle N(2)	C–S–N(2)–H(3)	H(3)–N(2)–N(1)–H(1)	H(3)–N(2)–N(1)–H(1)
MSH	120.2(2)	311(9)	347(4)	69(4)	165(4)	−97(7)
BUGXUM[a]	113.6	326.2	340.1	79.16	91.5	−26.8
JEHXOJ[a]	115.2		340.1	55.13		
PEZMEM[a,b]	112.4					
SEGLAR01[a,b]	100.0					
1[c]	113.3/	331.3/	338.9/	−154.9/−154.3	79.7/79.9	−42.9/−43.9
	114.0	332.6	339.4			
2[c]	116.8/	334.1/	349.3/	91.0/90.1	92.6/92.2	−34.4/−31.0
	117.6	332.3	350.0			
3[c]	111.7/	331.8/	334.5/	−63.6/−62.6	93.0/94.28	−29.3/−30.6
	112.3	333.7	335.1			
Dimer[d]	121.7	330.4	352.3	76.0	144.1	−95.0

[a] BUGXUM: 2-naphthylsulfonylhydrazine; JEHXOJ: benzenesulfonylhydraziniumphenylsulfonate; PEZMEM: 4-toluenesulfonylhydrazine; SEGLAR01: benzenesulfonylhydrazine. [b] The hydrogen atoms were not located. [c] The first and second values refer to the HF/6-31G(d) and HF/6-311++G(d,p) levels of calculation, respectively. [d] HF/6-311++G(d,p) level of calculation.

molHF/6-31G(d) level] are given in parentheses, the values being all relative to the most stable conformer **1** (or **1′**). In different conformers, the pyramidal groups $MeSO_2$ and $NHNH_2$ are staggered. In particular, the terminal units NH_2 and SO_2Me point in opposite directions with respect to the S–N(2) axis. The practicable pathways between the conformers and/or enantiomers are explicitly indicated by double-headed arrows.

In enantiomers **1** and **1′** the projection of the N(2)–H(3) linkage bisects the SO_2 moiety. Energetically, conformer **2** (or **2′**) lies *ca.* 3 kcal mol^{-1} above **1** (**1′**), but it is most similar to that of the experimental structure as the terminal NH_2 group is over the OSMe bisector and the N–N–S angle is quite open (117.6°). As shown in Table 4, the same angle is definitely smaller in the conformers **1** and **3** (114.0° and 112.3°, respectively). The relative energy of **3** and **3′** is highest (6.2 kcal mol^{-1}) because the terminal NH_2 group lies between the two oxygen atoms and the contacts between the nitrogen and oxygen lone pairs are short.

Isomer pairs **1**–**3** (or **1′**–**3′**) and **1**–**2** (or **1′**–**2′**) can interconvert by simple rotations about the S–N(2) bond *via* the eclipsed conformations of the pyramidal groups $MeSO_2$ and $NHNH_2$; the barriers to be overcome are 6.5 and 8.1 kcal mol^{-1}, respectively. In particular, the corresponding transition states **6** (or **6′**) and **5** (or **5′**) present the shortest contacts between non-hydrogen atoms (NH_2 group eclipsing one oxygen atom or the CH_3 group, respectively). Conversely, the direct interconversion **2** → **3** (or **2′** → **3′**) is impossible *via* an H/Me, NH_2/O eclipsed conformation (see below). In this case a two-step pathway is required and two barriers need to be crossed.

The interconversion between optical isomers always requires an "umbrella" inversion at the N(2) atom, occasionally accompanied by a rotation about the S–N(2) axis. While the **3** → **3′** interconversion proceeds through a single step (TS **7**), transit through a third isomer and the crossing of two consecutive barriers is needed to interconvert **1** into **1′** and **2** into **2′**. We present in some detail the various possibilities.

By considering the pair of most stable isomers **1** and **1′**, their direct interconversion would require a structure in which the most bulky groups CH_3 and NH_2 are eclipsed and the N(2) atom is planar: by imposing C_s symmetry, the latter species could be optimised (ΔE of *ca.* 10 kcal mol^{-1}) but it is not a true transition state as it has two imaginary frequencies. By visualising the modes of vibration, the more energetic one (-394.2 cm^{-1}) corresponds to the out-of-plane shift of the H atom bound to N(2), thus suggesting a natural rearrangement toward TS **5** (or **5′**). The second frequency (-184.8 cm^{-1}), which corresponds to the torsion of the NH–NH_2 group about the S–N vector, indicates an alternative preference for TS **4** (or **4′**). Evidently, the **1** → **1′** interconversion can follow either of the pathways **1** → **5** → **2** → **4** → **1′** or **1** → **4′** → **2′** → **5′** → **1′**. Since the TS **4** (or **4′**) implies a definitely smaller barrier than **5** or **5′** (3.2 *vs.* 8.1 kcal mol^{-1}), the latter pathway appears favoured.

The enantiomers **3** and **3′** are directly related by the transition state **7**, having C_s symmetry. The corresponding barrier (*ca.* 5 kcal mol^{-1}) is now halved with respect to the hypothetical barrier for the direct **1** → **1′** interconversion (TS with C_s symmetry) because of the reduced steric hindrance (CH_3 and H eclipsed).

The fact that no direct **2** → **2′** interconversion was detected is most likely due to the complex pathway, which combines N planarisation and molecular torsion about the S–N axis. Notice that in **3** → **3′**, the planarisation of nitrogen (TS **7**) is simply attained by moving the H atom, while in the **1** → **1′** conversion, the analogous movement of the NH_2 group is ruled out because of the two imaginary frequencies already pointed out. Since the **2** → **2′** path would require the simultaneous rearrangement of both H and NH_2 substituents, the direct interconversion appears most difficult. As shown by the sketches of Fig. 1, the possible intermediates are **1′** or **1**. Again, two alternative pathways are possible, namely **2** → **4** → **1′** → **5′** → **2′** or **2** → **5** → **1** → **4′** → **2′**. Given the differences between the barriers to be passed consecutively (0.3 and 8.1 *vs.* 8.1 and 3.2 kcal mol^{-1}), the first option appears more probable.

So far, we have underlined the energetics of conformers and enantiomers by focusing on the S–N torsion and the planarisation of the central N atom. In the presence of the hydrazine moiety it is important to evaluate the energetic cost of the N–N torsion as well. Accordingly, the potential energy surface was calculated for the combined rotations about the N(1)–N(2) and N(2)–S bonds. The corresponding contour map is presented in Fig. 3. It is characterised by two well-defined energy valleys at one given angular value for the O(1)–S–N(2)–N(1) torsion ($\tau_1 = -42°$). As expected, the deepest minimum corresponds to the isomer **1**, with the H2–N(1)–N(2)–S dihedral angle $\tau_2 = 85°$. In this case, the adjacent nitrogen lone pairs are in a *gauche* disposition and their repulsion is minimised in agreement with the results of other *ab initio* calculations for the hydrazine molecule itself.[21] A clockwise rotation about the N–N bond (τ_1 is fixed at $-42°$) causes a rapid increase in the energy (see Fig. 4). The energy maximum (at $\tau_2 = 0°$ with *syn* conformation) corresponds to an eclipsed conformation in which the nitrogen lone pairs are coplanar and closest to each other. In this case, the electron repulsion determines an energy barrier of *ca.* 15 kcal mol^{-1}. A

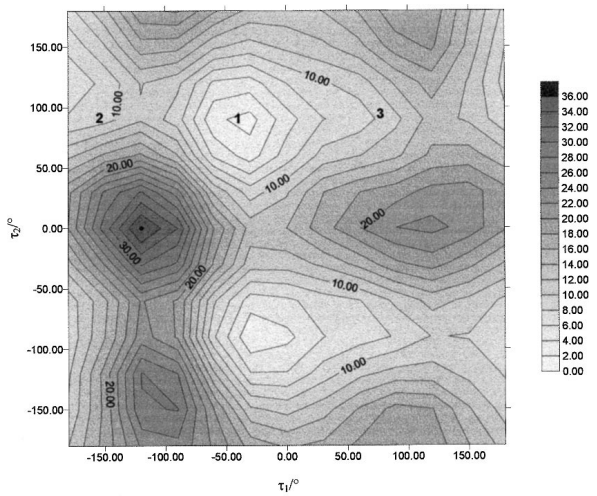

Fig. 3 Two-dimensional energy map [HF/6-31G(d) level] as a function of the two dihedral angles τ_1 [O(1)–S–N(2)–N(1)] and τ_2 [H(2)–N(1)–N(2)–S].

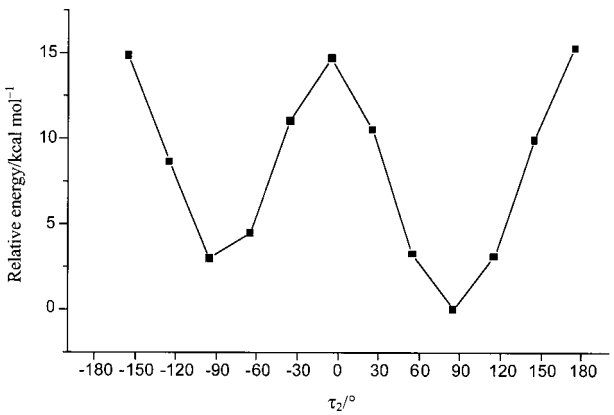

Fig. 4 Energy profile for the rotation about τ_2 [H(2)–N(1)–N(2)–S, $\tau_1 = -42°$] at the HF/6-31G(d) level.

further τ_2 rotation of 90° results in a new *gauche* disposition of the lone pairs and the energy is only *ca.* 3 kcal mol^{-1} higher than the global minimum. This small destabilising effect may be due to the terminal NH_2 unit, which points toward and not away from the $MeSO_2$ group. Finally, it is noteworthy that the conformations characterised by the *anti* disposition of the nitrogen lone pairs, $\tau_2 = \pm 180°$, are very destabilised (ΔE *ca.* 15 kcal mol^{-1}). The comparable destabilisations of both the *anti* and *syn* conformations may be justified by short contacts between each nitrogen lone pair and that of its adjacent oxygen atom.

The conformational energy profile for the τ_1 rotation about the S–N(2) vector (with $\tau_2 = 85°$) is shown in Fig. 5. It is easy to recognise all of the staggered minima (**1**, **2** and **3**) as well as the transition states **5** and **6**.

Since the TS for the direct interconversion **2** → **3** (or **2′** → **3′** in Fig. 1) was not detected by the usual Gaussian94 routines, it was assumed to be a two-step process, namely **2** → **1** followed by **1** → **3**. In the profile of Fig. 5, the highest peak (**8**, ΔE *ca.* 15 kcal mol^{-1}) corresponds to the eclipsed conformer with one oxygen atom and the hydrogen atom over the NH_2 and CH_3 groups, respectively. Obviously, the reliability of this structure as a true transition state cannot be proven and the associated high energy does not seem favourable. It is interesting to note that the energetics involved for torsions about the S–N(2) bond are about the same order of magnitude (at least 12 kcal mol^{-1}) as those found for the torsion about the N(1)–N(2) bond.

Energetics of hydrogen bonding in the dimer

The simplest way to evaluate the stabilisation associated with the dimerisation of MSH (as found in the crystal structure) is to subtract twice the energy of the optimised isomer **2** (the computed conformer closest to the observed one) from that of the optimised dimer. The result is *ca.* 5 kcal mol^{-1} (*i.e.*, *ca.* 2.5 kcal mol^{-1} per hydrogen bond). In order to estimate the associated basis set superposition error (BSSE),[22] two additional calculations were performed. In the first one, the atoms of a centrosymmetric half of the dimer were assigned nuclear charges equal to 0. Then, only a half dimer was actually calculated. The BSSE correction (1.02 kcal mol^{-1}) was simply obtained as twice the difference between the total energies from the two calculations. Essentially, the energy of each hydrogen bond is as small as 2 kcal mol^{-1} and an even smaller energy gain is associated with dimerisation if the most stable models **1** or **1′** are considered as reference points. Thus, it is not possible to conclude that the aggregation occurs in solution as well as in the solid state.

Analysis of the vibrational spectra

Since the X-ray structure of MSH shows that two molecules dimerise through hydrogen bonding, it is interesting to compare the IR spectra recorded from the solid as well as from the liquid (molten) state. The numerical data associated with both the IR and the Raman spectra are presented in Table 5. The differences between the IR spectra relative to the crystalline and molten compounds are not large, thus suggesting that the H-bonding may also be preserved in the melt. Since the two MSH molecules in the dimer are related by the centre of inversion, in the crystal each vibration of the isolated molecule is expected to be split, one vibration being IR active and the other Raman active. Thus, the observed differences in the wavenumbers of the corresponding IR and Raman bands may be explained.

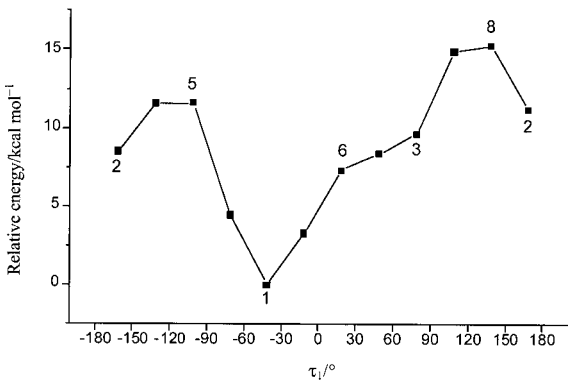

Fig. 5 Energy profile for the rotation about τ_1 [O(1)–S–N(2)–N(1), $\tau_2 = 85°$] at the HF/6-31G(d) level.

The proposed assignment of the IR and Raman bands of MSH (Table 5) was made taking into consideration the data reported in the literature for compounds that contain the same functional fragments, namely sulfonamides[23–27] and sufonylhydrazines,[28] methanesulfonyl derivatives,[29–32] hydrazines[33–38] and carboxylic acid hydrazides.[39–42] As a whole, these assignments are in agreement with the *ab initio* results (Table 5). Concerning the latter, the graphical user interface GaussView was used to display the vibrational modes based on the frequency calculation. For the H-bonded dimer the *ab initio* calculations predicted 30 pairs of bands corresponding to the intramolecular modes, and 6 additional bands in the lowest frequency range, which should be ascribed to the intramolecular vibrations. As it is known,[43] the *ab initio* calculations at the HF level overestimate the force constants, and hence the obtained vibrational frequencies are higher than the experimental ones. The usually applied correction factor of 0.89[44] does not allow us to reproduce precisely the experimental frequencies as the relative differences (before correction) vary between 6% and 35% (average 15%). Most importantly however, the sequence of computed vibrations coincides with experiment except for the following pairs of bands whose order is interchanged: $\delta(HN)/\delta_{as}(CH_3)$, $\nu(NN)/\nu_s(SO_2)$ and $\delta(CSN)/\tau(SO_2)$.

Another confirmation that the vibrations of MSH can be correctly assigned comes from NCA, also performed by us. As seen in Table 5, the splitting of the bands due to the formation of the H-bonded aggregate is rather small so that we could restrict the NCA calculation to only one isolated MSH molecule by imposing the same geometry as the dimer (see Table 2). The NCA wavenumbers and the corresponding potential energy distributions (PED) are also given in Table 5, while the optimised force field is defined in Table 6. The agreement with experimental wavenumbers is good, the RMS difference being 0.7%. A direct comparison between the force constants obtained from NCA and the literature data for some related molecules,[30–33,37,41] is perhaps not fully appropriate because of the differently defined force fields. Nevertheless, the values obtained for the MSH force constants appear to be in the expected range (see Table 6). Most of the vibrational bands of the CH_3SO_2N fragment are quite typical and their assignment is straightforward on the basis of the available literature data.[23–32] It is worth mentioning however that, according to the PED, an almost complete mixing of the CS and SN stretching vibrations takes place. Accordingly, rather than considering the bands at 850 and 764 cm^{-1} as "pure" ν(SN) and ν(CS) vibrations, a more reasonable assignment attributes these to the asymmetric and symmetric components of the CSN stretching. The visualisation of the vibrational modes associated with the corresponding frequencies obtained from the *ab initio* calculations $\tilde{\nu}$ 846 IR, 835 R for ν(SN) and $\tilde{\nu}$ 735 IR, 731 R for ν(CS)] fully confirms this assignment.

Special attention should be paid to the vibrations of the $SNHNH_2$ residue. In the IR spectrum of the acetonitrile solution, the NH_2 and NH stretching bands were observed at the following frequencies: 3380, 3276, 3193 and 3175 cm^{-1}. The wavenumbers of these bands appear to increase in going from solid state, to melt, to solution, an observation that can be explained in terms of decreasing molecular association. In

Table 5 Fundamental vibrations of $CH_3SO_2NHNH_2$ (in cm^{-1}): comparison between the experimental data, NCA[a] and *ab initio*[b] results

Experimental $\tilde{\nu}$				*Ab initio*		NCA		
IR solid	IR melt	Raman	Ave	$\tilde{\nu}$	δ, [c] (%)	$\tilde{\nu}$	PED[d] (%)	Assignment
3354 sh[e]		3366 m	3349	3814 R[f]	13.9	3349	100 ν(NH)	$\nu_{as}(NH_2)$[g]
3317 m	3358 m			3813 IR				
3277 m	3308 m	3298 w	3280	3773 IR	15.0	3280	100 ν(HN)	ν(HN)
	3263 m	3256 w		3769 R				
3136 m	3163 m		3175	3711 IR	16.9	3180	100 ν(NH)	$\nu_s(NH_2)$
		3226 w		3710 R				
3036 w	3023 w		3028	3307 IR	9.2	3023	99 ν(CH)	$\nu_{as}(CH_3)$
		3026 w		3307 R				
			3014	3298 IR	9.4	3019	100 ν(CH)	$\nu_{as}(CH_3)$
		3014 w		3298 R				
2935 w	2930 w		2933	3203 IR	9.2	2933	100 ν(CH)	$\nu_s(CH_3)$
		2934 m		3203 R				
		1639 w	1625	1839 R	13.1	1625	87 δ(HNH)	$\delta(NH_2)$
1617 m	1620 m			1836 IR				
1429 m	1424 sh		1426	1581 IR	10.9	1423	88 δ(HCH), 10 δ(HCS)	$\delta_{as}(CH_3)$
		1426 sh		1581 R				
1412 m	1409 m		1412	1571 IR	11.3	1415	90 δ(HCH)	$\delta_{as}(CH_3)$
		1414 m		1571 R				
		1395 sh	1395	1626 R	16.2	1396	33 δ(HNN), 34 δ(HNS),	δ(HN)
	1395 sh			1615 IR			16 ν(NN)	
1335 s	1332 s		1329	1499 IR	12.8	1329	34 δ(HCH), 52 δ(HCS),	$\delta_s(CH_3)$
		1320 w		1499 R			12 ν(CS)	
1318 s	1319 s		1310	1457 IR	11.2	1310	78 ν(SO)	$\nu_{as}(SO_2)$
		1292 w		1456 R				
1295 sh			1283	1438 IR	12.1	1285	90 δ(NNH)	$\tau(NH_2)$
		1270 w		1438 R				
		1147 sh	1154	1248 R	8.1	1155	67 ν(SO)	$\nu_s(SO_2)$
1158 s	1157 s			1246 IR				
		1132 s	1132	1314 R	15.9	1130	47 ν(NN), 18 δ(HNN),	ν(NN)
1130 sh	1135 sh			1310 IR			13 δ(HNS)	
994 sh	990 sh		992	1085 IR	9.4	986	89 δ(HCS)	$\rho(CH_3)$
				1085 R				
976 m	970 m		972	1078 IR	10.8	979	78 δ(HCS)	$\rho(CH_3)$
		971 w		1076 R				
937 m	935 sh		930	1067 IR	14.7	930	70 δ(NNH)	$\omega(NH_2)$
		917 w		1066 R				
850 m	844 m		849	951 IR	11.3	848	30 ν(SN), 29 ν(CS)	ν(SN)
		854 w		938 R				
764 m	760 m	729 w	742	826 IR	11.1	747	33 ν(CS), 23 ν(SN)	ν(CS)
		715 s		821 R				
650 m	640 m		625	699 IR	5.7	629	26 δ(HNN), 25 δ(HNS)	δ(HN)
		586 m		622 R				
529 s	527 s		527	595 IR	11.9	527	57 δ(OSO)	$\delta(SO_2)$
		526 w		584 R				
455 m	454 m		454	564 IR	24.2	458	33 δ(CSO), 29 δ(OSN),	$\omega(SO_2)$
		425 s		564 R			12 δ(SNN)	
			415	486 R	16.6	412	51 δ(CSO), 32 δ(OSN)	$\rho(SO_2)$
409 w	420 sh			482 IR				
		347 m	345	365 R	5.7	347	53 δ(CSO), 26 δ(OSN)	$\tau(SO_2)$
344 m	344 m			364 IR				
321 sh		322 w	318	435 IR	28.5	318	60 δ(CSN), 10 δ(CSO),	δ(CSN)
311 sh	316 sh			382 IR			10 δ(OSN)	
	265 sh	264 m	261	336 R	25.3	253	47 δ(OSN), 25 δ(SNN),	δ(SNN)
257 m	259 m			318 IR			14 t(NN)	
		238 w	215	267 R	21.9	216	63 t(NN), 13 δ(CSN),	t(NN)
203 w	203 w			257 IR			11 δ(SNN)	
		172 m	173	221 R	27.2	173	98 t(CS)	t(CS)
173 w	175 w			219 IR				
			97	132 IR	34.5	96	83 t(SN)	t(SN)
		97 m		129 R				
				112 R				Inter-
				62 R				molecular
				50 R				modes
				42 IR				
				33 IR				
				15 IR				

[a] The NCA results refer to a single molecule (see text). [b] The *ab initio* results refer to the H-bound dimer (see text). [c] δ (%) = 100 $[\tilde{\nu}(ave)_{ab\ initio} - \tilde{\nu}(ave)_{exptl}]/\tilde{\nu}(ave)_{exptl}$. [d] Potential energy distribution; contributions less than 10% are omitted. [e] Abbreviations: m = medium, s = strong, w = weak, sh = shoulder. [f] R and IR stand for Raman- and IR-active, respectively. [g] Notations: as = asymmetric, s = symmetric, t = torsional, δ = bending, ν = stretching, ρ = rocking, τ = twisting, ω = wagging.

Table 6 Internal coordinates and optimised force constants from the NCA of MSH

	Internal coordinate[a]	Force constant[b]
Stretching		
CH	CH(4), CH(5), CH(6)	4.887
CS	CS, SN(2)	3.890
SO	SO(1), SO(2)	8.968
NN	N(2)N(1)	5.792
HN	H(3)N(2)	5.937
NH	N(1)H(1), N(1)H(2)	5.889
Bending		
HCH	H(4)CH(5), H(4)CH(6), H(5)CH(6)	0.422
HCS	H(4)CS, H(5)CS, H(6)CS	0.647
CSO	CSO(1), CSO(2), O(1)SN(2), O(2)SN(2)	1.420
OSO	O(1)SO(2)	1.431
CSN	CSN(2), SN(2)N(1)	1.109
HNN	H(3)N(2)S, H(3)N(2)N(1)	0.715
NNH	N(2)N(1)H(1), N(2)N(1)H(2)	0.693
HNH	H(1)N(1)H(2)	0.736
Torsional		
t(CS)	Torsion around CS bond	0.055
t(SN)	Torsion around SN(2) bond	0.097
t(NN)	Torsion around N(2)N(1) bond	0.052
Off-diagonal		
CH–CH		0.038
CS–NN		0.162
SO–SO		0.358
NH–NH		−0.183
NN–HNN		0.110
HCH–HCH		−0.067
CSO–CSO		0.247
CSO–CSN		0.188
CSN–CSN		0.197
HNN–HNN		0.233
NNH–NNH		−0.145
HNH–NNH		0.100

[a] The atom numbering is according to Fig. 2. [b] Units: stretching and off-diagonal stretching–stretching are in mdyn $Å^{-1}$; bending and off-diagonal bending–bending are in mdyn Å rad^{-2} and off-diagonal stretching–bending are in mdyn rad^{-1}.

order to verify the assignments of the vibrational modes of the fragment $SNHNH_2$, we examined the IR spectrum of a partially deuterated sample of MSH, which probably contains a mixture of the non-deuterated, d_1, d_2 and d_3 derivatives. Upon deuteration, the $\nu_{as}(NH_2)$, $\nu(NH)$ and $\nu_s(NH_2)$ bands are shifted to 2469, 2426, 2406 and 2350 cm^{-1}, and the $\delta(ND_2)$ band appears as a shoulder at about 1195 cm^{-1} on the low-frequency contour of the strong $\nu_a(SO_2)$ band. The isotopic ratio $\tilde{\nu}_H/\tilde{\nu}_D$ for both groups of bands is 1.36, similar to other hydrazine derivatives.[36,37,39,40]

At variance with the $\nu(NH_2)$, $\nu(NH)$ and $\delta(NH_2)$ bands, the assignment of the remaining modes of the $SNHNH_2$ residue was complicated due to partial overlap with other bands. Moreover, the data for similar fragments in the literature are rather variable. A new band at 1032 cm^{-1} with a shoulder at 1049 cm^{-1} was registered in the spectrum of the deuterated sample, which should be ascribed to the DN bending vibration. Probably, the corresponding band in the spectrum of the non-deuterated species may be identified as the small shoulder on the $\delta_{as}(CH_3)$ band, which appears at 1395 cm^{-1}. The bands at 650, 640 and 586 cm^{-1} in the IR and Raman spectra of the non-deuterated MSH species were assigned to the second HN bending mode. The significant difference in the IR and Raman wavenumbers agrees with that predicted by the *ab initio* calculations. We could not identify the HN bending band in the IR spectrum of the deuterated sample as it is probably obscured by the relatively intense band of the SO_2 bending vibration. Our assignments for the δ(HN) δ(DN)] modes of MSH are in good agreement with the data of Hanai *et al.*[27] The literature data relative to the NNH bending modes of molecules containing the NNH_2 fragment are somewhat contradictory.[33,36,37,39,40] It is noteworthy that a similar situation occurs with respect to the analogous CNH vibrations in primary amines.[45–47] On the basis of our *ab initio* and NCA results, we ascribe the IR bands at 1295 (shoulder) and 937 cm^{-1} to the $\tau(NH_2)$ and $\omega(NH_2)$ vibrations, respectively. These values agree with those of Durig *et al.*[36] for methylhydrazine. In the IR spectrum of deuterated MSH, no band corresponding to that at 1295 cm^{-1} was detected as it is probably masked by the $\rho(CH_3)$ absorption around 990 cm^{-1}. However, an extra band at 796 cm^{-1} with a shoulder at 819 cm^{-1} corresponds most likely to that at 937 cm^{-1} appearing in the spectrum of the non-deuterated compound. Thus, the $\tilde{\nu}_H/\tilde{\nu}_D$ ratios for these two bands should be *ca.* 1.3 and 1.16, respectively, the values being close to the ratios of the corresponding bands in methylhydrazine.[36]

The literature data on the NN stretching vibration in hydrazine moieties also vary significantly (from *ca.* 870 to 1160 cm^{-1}).[33–37,39] On the basis of the calculations, the absorption at 1130 cm^{-1}, observed as a shoulder in the IR spectra and as a distinct band in the Raman spectrum of MSH, should be ascribed predominantly to the NN stretching vibration. This value is in accordance with the data of Durig *et al.*[36] and of Mashima.[39] As the PED revealed (Table 5), this mode is not purely NN stretching, and contains a considerable contribution from the δ(HN) vibration.

The bands of the intermolecular vibrations as predicted by the *ab initio* calculations (112–15 cm^{-1}) fall outside the range of the spectrometers used and we cannot comment on them.

Conclusion

This paper highlights the conformational properties of MSH in view of experimental and theoretical results. In the solid state, the conformers, which are pairwise aggregated, are not the most stable ones. Indeed, the theoretical analysis shows that there are a number of possible conformers and relative enantiomers and the pathways for their interconversion

(detection of transition states and associated energy barriers) have been outlined. Essentially, it appears that the torsion about the S–N and N–N vectors have comparable energy costs as well as the planarisation at the nitrogen atom bound to sulfur (transition states between enantiomers). For the latter type of rearrangement, it has been found that not all the direct pathways are practicable. The energy associated with MSH dimerisation *via* hydrogen bonding between hydrazine moieties has been estimated to be of the order of a couple of kcal mol^{-1}. This is a weak bond and it cannot be concluded that the dimer also exists in solution. However, the IR spectra (fully analysed by NCA) suggest that the dimer is likely to be maintained in the melt.

Acknowledgements

N.D. thanks the UNESCO Global Network for Molecular and Cell Biology for financial support (Grant No 436), as well as the NATO Scientific Affairs Division and the Scientific and Technical Research Council of Turkey (TÜBİTAK) for a fellowship. Thanks are due to the Area della Ricerca di Firenze for computational services provided (Dr. A. Tronconi and Mr. S. Cerreti).

References

1 A. Albert, *Selective Toxicity*, Chapman and Hall, London, New York, 1985.
2 N. R. Lomax and V. L. Narayanan, *Chemical Structures of Interest to the Division of Cancer Treatment*, Developmental Therapeutics Program, National Cancer Institute, Bethesda, MD, 1988, vol. VI.
3 S. Topiol, M. Sabio and P. W. Erhardt, *J. Chem. Soc., Perkin Trans. 2*, 1988, 437.
4 H. Rutner, N. Lewin, E. C. Woodbury, T. J. McBride and K. V. Rao, *Cancer Chemiother. Rep., Part 1*, 1974, **58**, 803.
5 A. G. Newcombe, *Can. J. Chem.*, 1955, **33**, 1250.
6 V. G. Dashevsky, *Konformatsionnyy Analiz Organicheskikh Molekul*, Khimiya, Moscow, 1982.
7 D. D. Perrin, W. F. F. Armarego and D. R. Perrin, *Purification of Laboratory Chemicals*, Pergamon Press, Oxford, 1980.
8 J. W. Powell and M. C. Whiting, *Tetrahedron*, 1959, **7**, 305.
9 A. Altomare, G. Cascarano, C. Giacovazzo and A. Guagliardi, *J. Appl. Crystallogr*, 1993, **26**, 343.
10 G. M. Scheldrick, *SHELX93, A Program for Crystal Structure Determination*, University of Gottingen, Germany, 1993.
11 D. T. Cromer and J. T. Waber, *Acta Crystallogr.*, 1965, **18**, 104.
12 M. J. Frisch, G. W. Trucks, H. B. Schlegel, P. M. W. Gill, B. G. Johnson, M. A. Robb, J. R. Cheeseman, T. A. Keith, G. A. Petersson, J. A. Montgomery, K. Raghavachari, M. A. Al-Laham, V. G. Zakrzewski, J. V. Ortiz, J. B. Foresman, J. Cioslowski, B. B. Stefanov, A. Nanayakkara, M. Challacombe, C. Y. Peng, P. Y. Ayala, W. Chen, M. W. Wong, J. L. Andres, E. S. Replogle, R. Gomperts, R. L. Martin, D. J. Fox, J. S. Binkley, D. J. Defrees, J. Baker, J. P. Stewart, M. Head–Gordon, C. Gonzalez and J. A. Pople, *Gaussian94*, Gaussian Inc., Pittsburgh, PA, 1995.
13 T. Sundius, *Documentation for the Program MOLVIB (Version 6.0)*, Department of Physics, University of Helsinki, Helsinki, 1991.
14 T. Sundius, *Commentat. Phys.-Math.*, 1977, **47**, 1.
15 T. Sundius, *J. Mol. Struct.*, 1990, **218**, 321.
16 G. V. Gridunova, V. E. Shklover, Y. T. Struchkov and B. A. Chayanov, *Cryst. Struct. Commun.*, 1982, **11**, 1879.
17 P. Lightfoot, M. Tremayne, C. Glidewell, K. D. M. Harris and P. G. Bruce, *J. Chem. Soc., Perkin Trans. 2*, 1993, 1625.
18 A. N. Chekhlov and I. V. Martyno, *Kristollografiya*, 1988, **33**, 1527.
19 J. N. Scholz, P. S. Engel, C. Glidewell and K. H. Whitmire, *Tetrahedron*, 1989, **45**, 7695.
20 (*a*) U. Buck, X. J. Gu, M. Hobein and C. Lauenstein, *Chem. Phys. Lett.*, 1989, **163,** 455; (*b*) U. Buck, X. J. Gu, M. Hobein, C. Lauenstein and A. Rudolph, *J. Chem. Soc., Faraday Trans.*, 1990, **86**, 1923.
21 (*a*) N. V. Riggs and L. Radom, *Aust. J. Chem.*, 1986, **39**, 1917; (*b*) H. B. Schlegel and A. Skancke, *J. Am. Chem. Soc.*, 1993, **115**, 7465.
22 S. F. Boys and F. Bernardi, *Mol. Phys.*, 1970, **19**, 533.
23 K. Hanai, T. Okuda, T. Uno and K. Machida, *Spectrochim. Acta, Part A*, 1975, **31**, 1217.
24 A. R. Katritzky and R. A. Jones, *J. Chem. Soc.*, 1960, 4497.
25 N. Bacon, A. J. Boulton, R. T. C. Brownlee, A. R. Katritzky and R. D. Topsom, *J. Chem. Soc.*, 1965, 5230.
26 Y. Tanaka and Y. Tanaka, *Chem. Pharm. Bull.*, 1965, **13**, 858.
27 K. Hanai, A. Noguchi and T. Okuda, *Spectrochim. Acta, Part A*, 1978, **34**, 771.
28 R. J. W. Cremlyn and D. N. Waters, *J. Chem Soc., Suppl. 2*, 1964, 6243.
29 R. D. McLachlan and V. B. Carter, *Spectrochim. Acta, Part A*, 1970, **26**, 1121.
30 T. Uno, K. Machida and K. Hanai, *Spectrochim. Acta, Part A*, 1971, **27**, 107.
31 G. Geiseler and G. Hanschmann, *J. Mol. Struct.*, 1971, **8**, 293.
32 G. Chassaing, J. Corset and J. Limouzi, *Spectrochim Acta, Part A*, 1981, **37**, 721.
33 J. S. Ziomek and M. D. Zeidler, *J. Mol. Spectrosc.*, 1963, **11**, 163.
34 L. Sacconi and A. Sabatini, *J. Inorg. Nucl. Chem.*, 1963, **25**, 1389.
35 A. Braibanti, F. Dallavalle, M. A. Pellinghelli and E. Leporati, *Inorg. Chem.*, 1968, **7**, 1430.
36 J. R. Durig, W. C. Harris and D. W. Wertz, *J. Chem. Phys.*, 1969, **50**, 1449.
37 D. P. Dowling and W. K. Glass, *Spectrochim. Acta, Part A*, 1988, **44**, 1351.
38 J. R. Durig, N. E. Lindsay and P. Groner, *J. Phys. Chem.*, 1989, **93**, 593.
39 M. Mashima, *Bull. Chem. Soc. Jpn.*, 1962, **35**, 1882.
40 M. Mashima, *Bull. Chem. Soc. Jpn.*, 1963, **36**, 210.
41 Y. Y. Kharitonov and R. I. Machkhoshvili, *Zh. Neorg. Khim.*, 1971, **16**, 1203.
42 R. I. Machkhoshvili, D. P. Metreveli, G. S. Mitaishvili and R. N. Shchelokov, *Zh. Neorg. Khim.*, 1985, **30**, 676.
43 A. Hinchliffe, *Computational Quantum Chemistry*, J. Wiley and Sons, New York, 1988.
44 J. B. Foresman and Æ. Frisch, *Exploring Chemistry with Electronic Structure Methods*, Gaussian Inc., Pittsburgh, PA, USA, 1993.
45 J. E. Stewart, *J. Chem. Phys.*, 1959, **30**, 1259.
46 E. L. Wu, G. Zerbi, S. Califano and B. Crawford, Jr., *J. Chem. Phys.*, 1961, **35**, 2060.
47 J. R. Durig, S. F. Bush and F. G. Baglin, *J. Chem. Phys.*, 1968, **49**, 2106.

Paper 9/06264E